


Article

Magnetic and Magnetostrictive Behaviors of Laves-Phase Rare-Earth—Transition-Metal Compounds $Tb_{1-x}Dy_xCo_{1.95}$

Chao Zhou ^{1,*}, Kaili Li ¹, Yuanliang Chen ¹, Zhiyong Dai ¹, Yu Wang ¹, Liqun Wang ¹, Yoshitaka Matsushita ² , Yin Zhang ¹, Wenliang Zuo ¹, Fanghua Tian ¹, Adil Murtaza ¹ and Sen Yang ^{1,*}

¹ School of Physics, MOE Key Laboratory for Nonequilibrium Synthesis and Modulation of Condensed Matter, Xi'an Jiaotong University, Xi'an 710049, China; likaaili2013@stu.xjtu.edu.cn (K.L.); xajtcyl@stu.xjtu.edu.cn (Y.C.); daizhiyong@stu.xjtu.edu.cn (Z.D.); yuwang@xjtu.edu.cn (Y.W.); wanglq@xjtu.edu.cn (L.W.); yzhang18@xjtu.edu.cn (Y.Z.); zuowenliang@xjtu.edu.cn (W.Z.); tth2017@xjtu.edu.cn (F.T.); adilmurtaza91@xjtu.edu.cn (A.M.)

² National Institute for Materials Science, Tsukuba 305-0047, Ibaraki, Japan; matsushita.yoshitaka@nims.go.jp

* Correspondence: chao.zhou@xjtu.edu.cn (C.Z.); yang.sen@xjtu.edu.cn (S.Y.)

Abstract: The magnetic morphotropic phase boundary (MPB) was first discovered in Laves-phase magnetoelastic system Tb–Dy–Co alloys (PRL 104, 197201 (2010)). However, the composition-dependent and temperature-dependent magnetostrictive behavior for this system, which is crucial to both practical application and the understanding of transitions across the MPB, is still lacking. In this work, the composition-dependence and temperature-dependence of magnetostriction for $Tb_{1-x}Dy_xCo_{1.95}$ ($x = 0.3\sim 0.8$) are presented. In a ferrimagnetic state (as selected 100 K in the present work), the near-MPB compositions $x = 0.6$ and 0.7 , exhibit the largest saturation magnetization M_S and the lowest coercive field H_C ; by contrast, the off-MPB composition $x = 0.5$, exhibits the largest magnetostriction, the lowest M_S , and the largest H_C . Besides, a sign change of magnetostriction is observed, which occurs with the magnetic transition across the MPB. Our results suggest the combining effect from the lattice strain induced from structure phase transition, and the influence of the MPB on magnetocrystalline anisotropy. This work may stimulate the research interests on the transition behavior around the MPB and its relationship with physical properties, and also provide guidance in designing high-performance magnetostrictive materials for practical applications.

Keywords: morphotropic phase boundary; magnetostriction; Laves-phase; temperature dependence; composition dependence



Citation: Zhou, C.; Li, K.; Chen, Y.; Dai, Z.; Wang, Y.; Wang, L.; Matsushita, Y.; Zhang, Y.; Zuo, W.; Tian, F.; et al. Magnetic and Magnetostrictive Behaviors of Laves-Phase Rare-Earth—Transition-Metal Compounds $Tb_{1-x}Dy_xCo_{1.95}$. *Materials* **2022**, *15*, 3884. <https://doi.org/10.3390/ma15113884>

Academic Editor: Israel Felner

Received: 3 May 2022

Accepted: 24 May 2022

Published: 29 May 2022

Publisher's Note: MDPI stays neutral with regard to jurisdictional claims in published maps and institutional affiliations.



Copyright: © 2022 by the authors. Licensee MDPI, Basel, Switzerland. This article is an open access article distributed under the terms and conditions of the Creative Commons Attribution (CC BY) license (<https://creativecommons.org/licenses/by/4.0/>).

1. Introduction

Magnetostrictive materials can realize the conversion between magnetic energy and mechanical energy, thus they are widely used in the key components of sensors, actuators, and transducers [1]. Due to the 3d–4f exchange interactions [2], many Laves-phase rare-earth-transition-metal compounds (RT_x, R denotes the rare-earth elements and T denotes the transition-metal elements, $x = 1.8\sim 2$) exhibit giant magnetostriction, e.g., TbFe₂, DyFe₂, TbCo₂, and DyCo₂ [3,4].

In 2010, Yang et al. reported the magnetic morphotropic phase boundary (MPB) in a Laves-phase pseudo-binary $Tb_{1-x}Dy_xCo_2$ system [5]. Later on, Bergstrom et al. reported the MPB in the classic system-Terfenol-D [6]. Afterwards, MPBs were discovered in more and more Laves-phase systems such as Tb–Gd–Co, Tb–Gd–Fe, Tb–Nd–Co, etc. [7–9]. The transition at the MPB involves not only the change of magnetic ordering, but also the change of structural ordering, thus yielding exotic magnetoelastic and magnetocaloric properties [10–13].

In practical applications, temperature variation is inevitable and impact on the properties of the magnetostrictive materials, so will influence the performance of the devices (sensors, actuators, and transducers). Although MPB has been utilized to realize large

magnetostriction, it is not only composition-dependent but also temperature-dependent. Whether one magnetostrictive material fits for an application, is determined not only by its maximum magnetostriction, but also by the temperature-dependent performance [14]. In view of this point, the MPB composition might not be the best candidate for application.

For a certain magnetostrictive material system, to optimize the composition to meet the application requirements, it is necessary to acquire both the temperature-dependence and composition-dependence of magnetostriction. For the proto magnetic MPB system-Tb-Dy-Co alloys, despite much intense research, e.g., spin reorientation behavior [15], magnetocaloric effect [16], the nature of transition [17], and the role of the electronic structure based on first principle calculation [18], investigation on the temperature-dependence and composition-dependence of magnetostriction, as well as the relation between the changing trend with MPB, is still lacking. Thus, we proposed to clarify the composition and temperature-dependent magnetostrictive behaviors in the MPB-involved systems.

In this work, for the Tb-Dy-Co system, the magnetostrictive behavior as a function of temperature and composition were investigated and discussed regarding the composition-dependence of magnetic properties, e.g., magnetization, coercive field, and magnetic susceptibility.

2. Materials and Methods

It is noticed that reducing the content of transition metal favors the formation of the Laves-phase compound [19–21], so the formula of stoichiometry is fixed to be $Tb_{1-x}Dy_xCo_{1.95}$ ($x = 0.3\sim 0.8$). The $Tb_{1-x}Dy_xCo_{1.95}$ alloy samples were prepared by arc melting method with the raw materials of Tb (99.9%), Dy (99.9%), and Co (99.9%) in argon atmosphere. In order to guarantee the composition homogeneity, the magnetic stirring was employed during the arc melting process and all ingots were melted six times. Samples used for physical property measurements are polycrystalline. The crystal structure was examined by X-ray diffraction (XRD, Bruker D8 ADVANCE, Hamburg, Germany) using Cu K α radiation ($\lambda = 0.154056$ nm) with an angle (2θ) step of 0.02° between 20° and 80° . The line scans of chemical elements were performed by scanning electron microscopy (SEM, JSM-7000F, JEOL, Tokyo, Japan). The chemical compositions were analyzed using X-ray fluorescence (XRF, Bruker S8 Tiger, Hamburg, Germany). The magnetization (M) versus magnetic field (H) hysteresis loops, and the magnetic susceptibility (χ) versus temperature (T) curves were measured using superconducting quantum interference device (SQUID, Quantum Design, Santa Barbara, CA, USA). The magnetostriction at the field of 20 kOe from 10 K to 130 K, was measured by the standard strain gauge technique with a gauge factor of $2.11 \pm 1\%$, combined with the temperature controlling system (Cryostat Device, Cambridge, UK).

3. Results and Discussion

3.1. Crystal Structure Characterization

The XRD profiles for the selected compositions ($x = 0.3\sim 0.8$) at room temperature (~ 298 K) are shown in Figure 1a. All of the samples possess a pure C15 cubic Laves-phase structure (space group $Fd\bar{3}m$) [22], without any second phase (RT_3) that usually appears in Laves-phase rare-earth-transition metal alloys [23–25]. Figure 1b plots the corresponding crystal structure. It should be noted that when the temperature is below the Curie temperature T_C , the non-cubic structure symmetry can be detected using neutron diffraction or synchrotron XRD [5,26–28].

The line scans of elements using SEM (Figure S1 in the Supplementary Material), suggest the compositional homogeneity for all the available samples. It is also necessary to point out that the microstructure, i.e., the grain size, of Laves-phase intermetallic compounds usually does not play the key role for magnetic properties [29]. The comparison between the chemical relative mass percentages from the experiment and calculation (XRF results; Figure S2 in the Supplementary Material) reveals the consistence as the content of Dy increases. The deviation might stem from the loss in the arc-melting procedure.

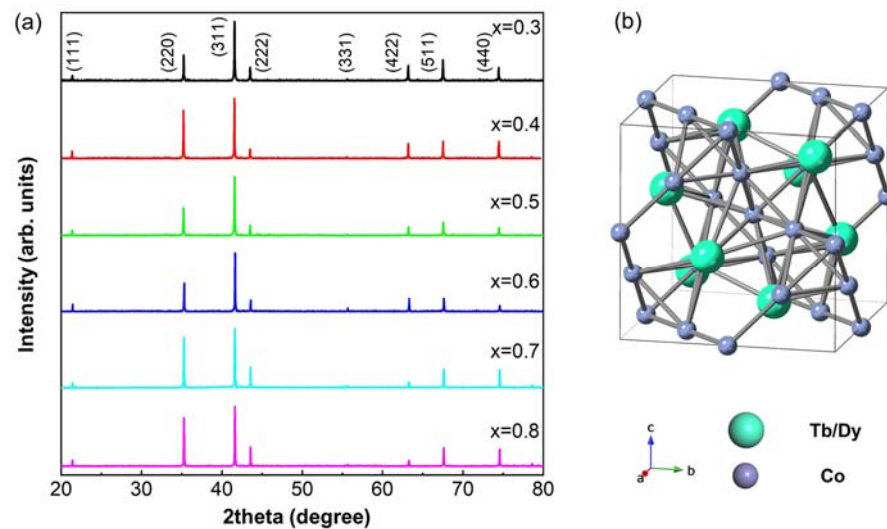


Figure 1. (a) X-ray diffraction profiles of $Tb_{1-x}Dy_xCo_{1.95}$ alloys ($x = 0.3, 0.4, 0.5, 0.6, 0.7, 0.8$), (b) the crystal structure of Laves-phase $Tb_{1-x}Dy_xCo_{1.95}$ alloys.

3.2. Temperature Spectrum of Magnetic Susceptibility and Magnetic Phase Diagram

The susceptibility versus temperature curves χ -T are shown in Figure 2(a1–a6) (the inverse susceptibility versus temperature curves $1/\chi$ -T can be referred to in Figure S3). Tb-rich composition (i.e., $x = 0.3$) and Dy-rich composition (i.e., $x = 0.8$) exhibit only one peak that denotes the paramagnetic–ferrimagnetic phase transition. The samples of the intermediate composition range (i.e., $x = 0.4\sim 0.7$) show two peaks, of which the one appearing at the higher temperature indicates the paramagnetic–ferrimagnetic transition and the one appearing at the lower temperature indicates the ferrimagnetic–ferrimagnetic transition. As proposed from the previous research work [5,27,30], the easy magnetization axis (EMA) of Tb-rich compositions aligns along [111], while that of the Dy-rich compositions aligns along [001]. Such a ferrimagnetic–ferrimagnetic transition is coined as the spin reorientation transition (SRT) [31].

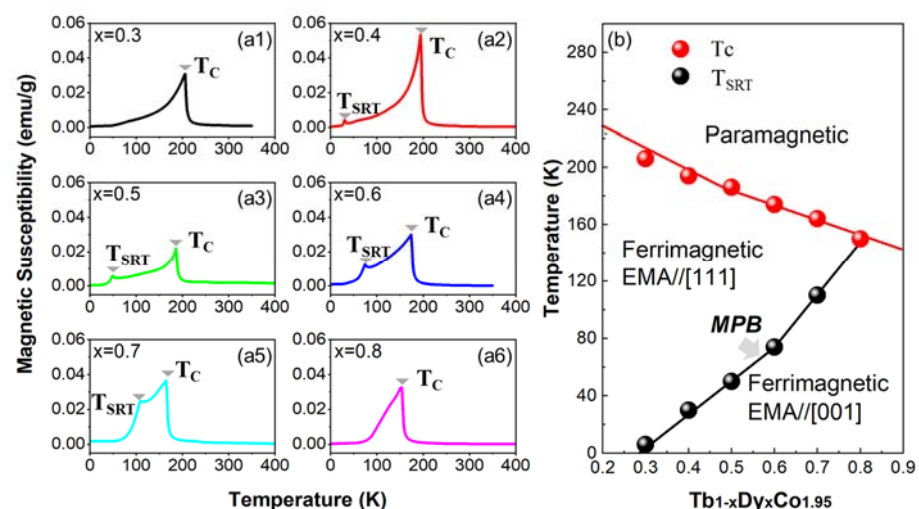


Figure 2. (a1–a6) Magnetic susceptibility versus temperature curves and (b) the phase diagram of $Tb_{1-x}Dy_xCo_{1.95}$.

Based on the EMA for two end members and the phase transition temperatures determined from the χ -T curves, the magnetic phase diagram is illustrated in Figure 2b. It can be seen that the MPB derives from the triple-point (the intersection point of the T_C line and the ferrimagnetic (EMA//[111])–ferrimagnetic (EMA//[001]) phase boundary). Since

the magnetocrystalline anisotropic coefficient K_1 values of Tb^{3+} ions and Dy^{3+} ions are negative and positive [32], respectively, the spin reorientation transition temperature T_{SRT} depends on the Tb/Dy ratio. With the increasing content of Dy, the T_C decreases while the T_{SRT} increases; the former is attributed to the less strength of the 3d–4f coupling between Dy and Co [33], and the latter is attributed to the enhanced 3d–4f–5d hybridization [34].

3.3. M - H Hysteresis Loops

To study the composition dependence of magnetic properties across the MPB, the measurement temperature is usually fixed at below the T_C [5], i.e., 100 K at the present work. The M - H hysteresis loops at 100 K are shown in Figure 3(a1–a6). The composition dependence of coercive field H_C and the saturation magnetization M_S (calculated using the law of approach to saturation [35]) are shown in Figure 3(b1,b2).

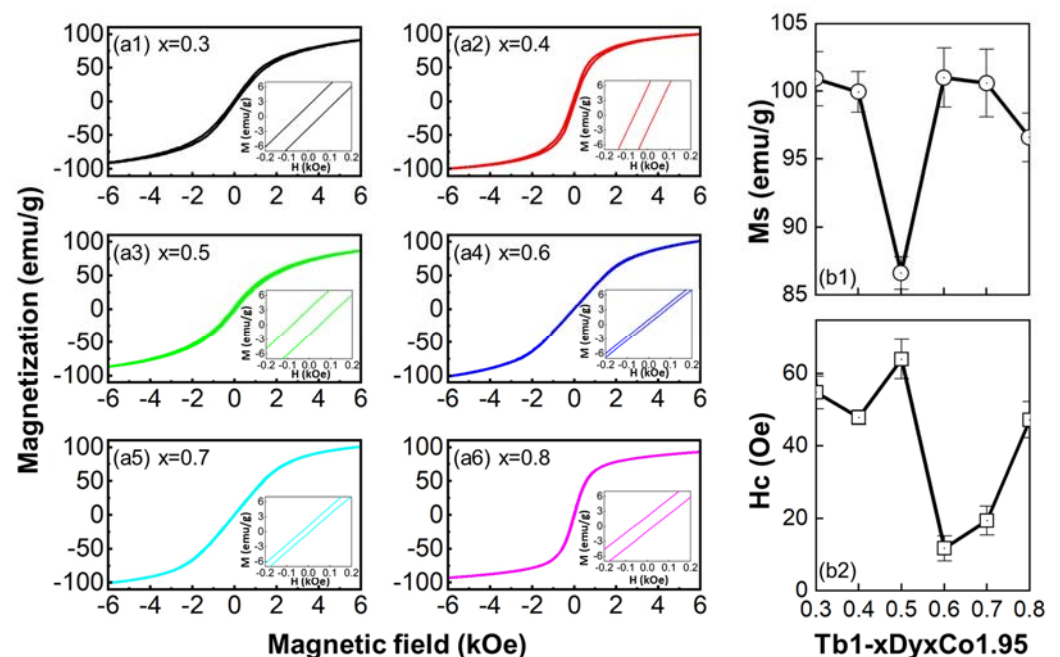


Figure 3. (a1–a6) Magnetization (M) versus Magnetic field (H) hysteresis loops of $Tb_{1-x}Dy_xCo_{1.95}$ alloys ($x = 0.3, 0.4, 0.5, 0.6, 0.7, 0.8$); Composition dependence of saturation magnetization M_S (b1) and coercive field H_C (b2) at 100 K.

The magnetic properties of Laves-phase rare earth—transition metal compounds, are dominated by the highly anisotropic rare earth sublattice, especially the distortion of the spherical 4f charge density of the rare earth sublattice [36]. As for the Tb–Dy–Co system, at a certain temperature, the anisotropic coefficient is definitely composition-dependent. Because of the differences of the 4f electron configurations in Tb^{3+} ($4f^8$) and Dy^{3+} ($4f^9$), the magnetic properties (M_S , H_C , etc.) exhibit a competition effect from both the Tb-sublattice and the Dy-sublattice. The compositions $x = 0.6$ and 0.7 , both locating close to the MPB (where the compensation of anisotropy occurs at T_{SRT}), exhibit a large M_S and a low H_C , which is attributed to the facility of magnetic domain switching resulted from the low magneto-crystalline anisotropy and low energy barrier at the MPB [37,38]. By contrast, the composition $x = 0.5$, which locates further to the MPB than $x = 0.6$ and 0.7 , shows the lowest M_S and the largest H_C , reflecting the competition effect from both the Tb-sublattice and the Dy-sublattice that reaches the extreme at $x = 0.5$. For 0.3 and 0.4, the Tb-sublattice is believed to play the dominant role.

3.4. Composition- and Temperature-Dependent Magnetostriction

Figure 4a shows the magnetostriction (ϵ) curves of $x = 0.3$ – 0.8 in the temperature range from 10 K to 130 K. For $x = 0.3, 0.4$, and 0.5 , ϵ remains positive and increases monotonously

with the decrease in temperature. For $x = 0.6, 0.7,$ and 0.8 , ϵ exhibits positive values at higher temperatures and negative values at lower temperatures. The T_{SRT} of $x = 0.3$ is ~ 6 K (the signal is too weak so that it cannot be clearly seen on Figure 2(a1)), out of the temperature region of 10 K~130 K. Within this temperature region, $x = 0.3$ possesses a rhombohedral phase (EMA// $[111]$), so exhibits positive magnetostriction.

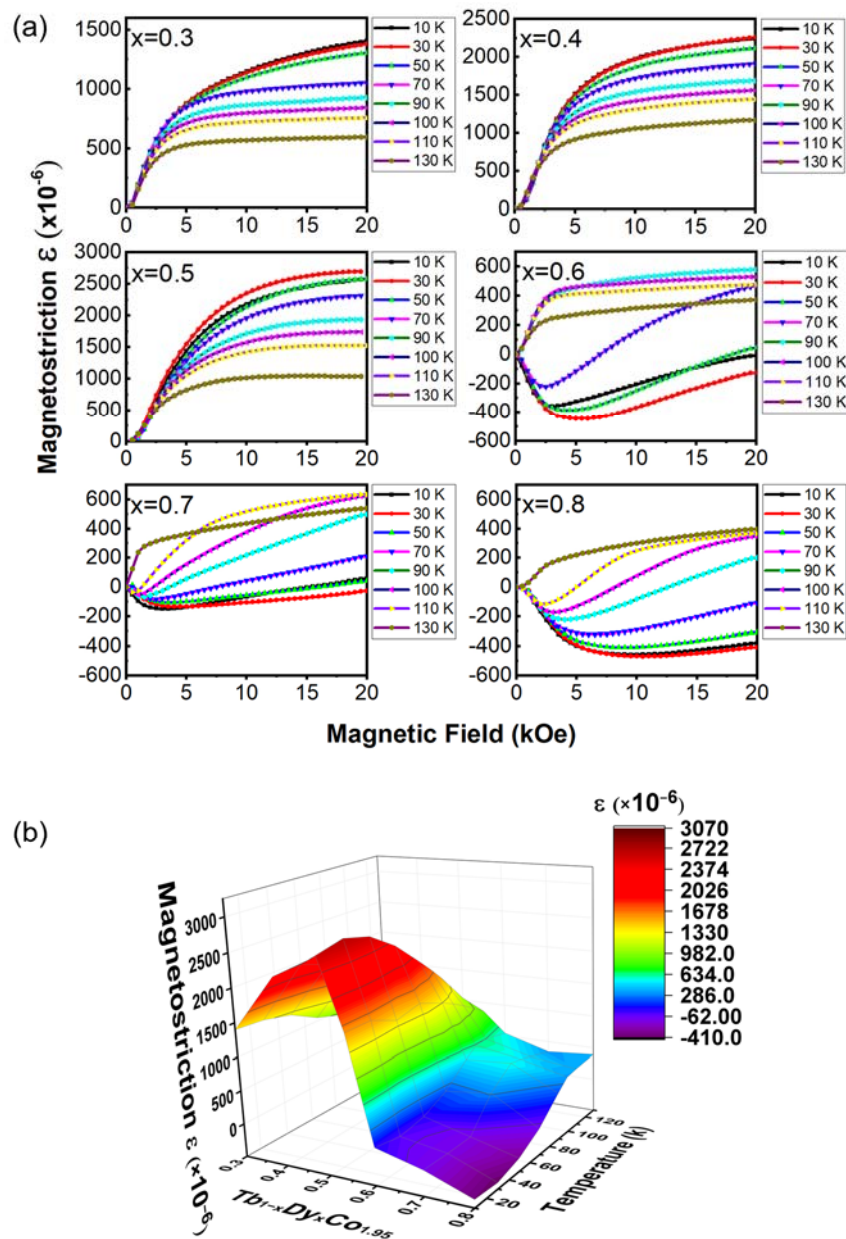


Figure 4. (a) Temperature-dependent magnetostriction curves of $\text{Tb}_{1-x}\text{Dy}_x\text{Co}_{1.95}$ alloys ($x = 0.3, 0.4, 0.5, 0.6, 0.7, 0.8$), (b) 3-dimensional diagrams of the magnetostriction as a function of composition and temperature.

Given that the transitions of Laves-phase intermetallics involve not only magnetic ordering but structural change, the magnetostriction, which originates from magnetoelastic coupling, can be well interpreted using a domain switching mechanism [5,27]. Based on the model proposed by Yang et al. [27], the magnetostriction is proportional to the lattice strain, which arises from the structural transition of magnetic materials. And conversely, the sign change of the measured magnetostriction indicates the change of crystal structure symmetry [14]. Moreover, the crystal structure symmetry conforms to the spontaneous

magnetization M_S direction (consistent with the EMA) [27]. Therefore, the sign change of ϵ for $x = 0.6, 0.7$ and 0.8 demonstrates both magnetic transition between two different ferrimagnetic phases (EMA//[111] and EMA//[001]), and concurring structure transition between rhombohedral and tetragonal phases [14,27]. It should be paid attention to that, the T_{SRT} of $x = 0.4$ and 0.5 lie within the temperature range of $10\text{ K}\sim 130\text{ K}$ (Figure 2b), but their magnetostrictions remain positive. This may be ascribed to the transition route at the MPB under the large external magnetic field, which is determined by the degree of magnetic ordering of two end members that form magnetic MPB [9].

Figure 4b shows the contour diagram of ϵ as a function of composition and temperature. For comparison, the magnetic properties of the current system are compared with those of the previously reported $Tb_{1-x}Dy_xCo_2$ system, as shown in Table 1. The composition-dependent sign change of the magnetostriction, together with the phase diagram (Figure 2), suggest that ϵ is influenced mainly by two factors: (1) the facility of magnetic domain switching as discussed above and (2) the theoretical saturated strain that is determined by the lattice strain [27]. The composition $x = 0.5$, located further away from the MPB (where the magneto-crystalline anisotropy of two end members compensate) [14], possesses a larger magneto-crystalline anisotropy than $x = 0.6$ and 0.7 . Meanwhile, $x = 0.5$ locates closer to the end member of $TbCo_2$, so it possesses a larger lattice strain upon domain switching, which results from the switching of the distorted rhombohedral lattice [27]. This observation is consistent with that reported in another MPB-involved system $Tb_{1-x}Dy_xFe_2$ [39]. Interestingly, such a phenomenon was also observed recently in a ferroelectric MPB-involved system [40].

Table 1. Comparison of magnetic properties between selected compositions of $Tb_{1-x}Dy_xCo_{1.95}$ and $Tb_{1-x}Dy_xCo_2$ systems.

Composition	M_S (emu/g)	H_C (Oe)	ϵ (ppm) at 110 K	Figure of Merit $ \epsilon /H_C$ ($Oe^{-1}\cdot 10^6$)	Reference
$Tb_{0.6}Dy_{0.4}Co_{1.95}$	99.9	47.9	1441	30.1	The present study
$Tb_{0.5}Dy_{0.5}Co_{1.95}$	86.6	64	1523	23.8	The present study
$Tb_{0.4}Dy_{0.6}Co_{1.95}$	101.1	11.7	475	40.6	The present study
$Tb_{0.3}Dy_{0.7}Co_{1.95}$	100.6	19.4	635	32.7	The present study
$Tb_{0.6}Dy_{0.4}Co_2$	115	102	1410	13.8	Ref. [5]
$Tb_{0.3}Dy_{0.7}Co_2$	105.5	15.6	828	53.1	Ref. [5]

4. Conclusions

In conclusion, the magnetic and magnetostrictive properties of $Tb_{1-x}Dy_xCo_{1.95}$ ($x = 0.3\sim 0.8$) alloys were systematically studied. The results reveal that the magnetic properties (M_S and H_C) are strongly influenced by the MPB, while the magneto-elastic property (ϵ) relies mainly on the composition-dependent crystal lattice distortion. Therefore, the off-MPB composition with EMA//[111], i.e., $x = 0.5$, exhibits the largest ϵ , the largest H_C , and the lowest M_S ; by contrast, the near-MPB compositions $x = 0.6$ and 0.7 exhibit the largest M_S and the lowest H_C , as well as a lower ϵ , compared with $x = 0.5$ and other Tb-rich compositions. Our work demonstrates the temperature-dependence and composition-dependence of magnetostriction for the proto magnetic MPB system Tb–Dy–Co and may accelerate the design of optimum magnetostrictive materials for energy conversion devices.

Supplementary Materials: The following supporting information can be downloaded at: <https://www.mdpi.com/article/10.3390/ma15113884/s1>, Figure S1: The line scans of chemical elements for $Tb_{1-x}Dy_xCo_{1.95}$ alloys and the corresponding element distribution (Tb, Dy, Co) for each composition ($x = 0.3, 0.4, 0.5, 0.6, 0.7, 0.8$); Figure S2: The X-ray Fluorescence (XRF) results for $Tb_{1-x}Dy_xCo_{1.95}$ alloys ($x = 0.3, 0.4, 0.5, 0.6, 0.7, 0.8$). Figure S3: The inverse susceptibility $1/\chi$ versus temperature curves above T_C for $Tb_{1-x}Dy_xCo_{1.95}$ alloys ($x=0.3, 0.4, 0.5, 0.6, 0.7, 0.8$).

Author Contributions: Conceptualization, C.Z. and S.Y.; experimental work, data acquisition, and analysis, K.L., Y.C., Z.D., L.W., Y.M., Y.Z., W.Z., F.T. and A.M.; writing—original draft preparation, K.L., Y.W. and C.Z.; writing—review and editing, Y.W.; project administration, S.Y.; funding acquisition, S.Y. All authors have read and agreed to the published version of the manuscript.

Funding: This research was funded by the National Key R&D Program of China (Grant Number 2021YFB3501401), the National Natural Science Foundation of China (Grant Numbers 91963111, 51601140), Key Scientific and Technological Innovation Team of Shaanxi Province (Grant Number 2020TD-001), Innovation Capability Support Program of Shaanxi (Grant Numbers 2018PT-28, 2017KTPT-04), the Fundamental Research Funds for the Central Universities (China) and the World-Class Universities (Disciplines), the Characteristic Development Guidance Funds for the Central Universities (China).

Informed Consent Statement: Not applicable.

Data Availability Statement: Not applicable.

Conflicts of Interest: The authors declare no conflict of interest.

References

1. O’Handley, R.C. *Modern Magnetic Materials: Principles and Applications*; John Wiley & Sons, Inc.: New York, NY, USA, 1999.
2. Duc, N.H.; Brommer, P.E. Formation of 3d-Moments and Spin Fluctuations in the Rare Earth—Transition Metal Intermetallics. In *Advanced Magnetism and Magnetic Materials*; Duc, N.H., Ed.; Vietnam National University Press: Hanoi, Vietnam, 2014; pp. 97–270.
3. Lee, E.W.; Pourarian, F. Magnetoelastic properties of (Rare-Earth)—Co₂ compounds. II. The anisotropic magnetostriction. *Phys. Status Solidi (A)* **1976**, *34*, 383–390. [[CrossRef](#)]
4. Clark, A.E.; Belson, H.S. Giant Room-Temperature Magnetostrictions in TbFe₂ and DyFe₂. *Phys. Rev. B* **1972**, *5*, 3642–3644. [[CrossRef](#)]
5. Yang, S.; Bao, H.; Zhou, C.; Wang, Y.; Ren, X.; Matsushita, Y.; Katsuya, Y.; Tanaka, M.; Kobayashi, K.; Song, X.; et al. Large Magnetostriction from Morphotropic Phase Boundary in Ferromagnets. *Phys. Rev. Lett.* **2010**, *104*, 197201. [[CrossRef](#)] [[PubMed](#)]
6. Bergstrom, R., Jr.; Wuttig, M.; Cullen, J.; Zavalij, P.; Briber, R.; Dennis, C.; Garlea, V.O.; Laver, M. Morphotropic Phase Boundaries in Ferromagnets: Tb_{1-x}Dy_xFe₂ Alloys. *Phys. Rev. Lett.* **2013**, *111*, 017203. [[CrossRef](#)] [[PubMed](#)]
7. Murtaza, A.; Yang, S.; Zhou, C.; Chang, T.; Chen, K.; Tian, F.; Song, X.; Suchomel, M.R.; Ren, Y. Anomalous magnetoelastic behaviour near morphotropic phase boundary in ferromagnetic Tb_{1-x}Nd_xCo₂ system. *Appl. Phys. Lett.* **2016**, *109*, 052904. [[CrossRef](#)]
8. Adil, M.; Yang, S.; Mi, M.; Zhou, C.; Wang, J.; Zhang, R.; Liao, X.; Wang, Y.; Ren, X.; Song, X.; et al. Morphotropic phase boundary and magnetoelastic behaviour in ferromagnetic Tb_{1-x}Gd_xFe₂ system. *Appl. Phys. Lett.* **2015**, *106*, 132403. [[CrossRef](#)]
9. Zhou, C.; Ren, S.; Bao, H.; Yang, S.; Yao, Y.; Ji, Y.; Ren, X.; Matsushita, Y.; Katsuya, Y.; Tanaka, M.; et al. Inverse effect of morphotropic phase boundary on the magnetostriction of ferromagnetic Tb_{1-x}Gd_xCo₂. *Phys. Rev. B* **2014**, *89*, 100101. [[CrossRef](#)]
10. Zhao, H.; Ji, Y.; Ma, T.; Fang, M.; Hao, Y.; Yang, T.; Zhou, C.; Yang, S.; Ren, X. Exceptional combination of large magnetostriction, low hysteresis and wide working temperature range in (1-x)TbFe₂-xDyCo₂ alloys. *Acta Mater.* **2021**, *220*, 117308. [[CrossRef](#)]
11. Hu, J.; Lin, K.; Cao, Y.; Yu, C.; Li, W.; Huang, R.; Fischer, H.E.; Kato, K.; Song, Y.; Chen, J.; et al. Adjustable Magnetic Phase Transition Inducing Unusual Zero Thermal Expansion in Cubic RCo₂-Based Intermetallic Compounds (R = Rare Earth). *Inorg. Chem.* **2019**, *58*, 5401–5405. [[CrossRef](#)]
12. Song, Y.; Chen, J.; Liu, X.; Wang, C.; Zhang, J.; Liu, H.; Zhu, H.; Hu, L.; Lin, K.; Zhang, S.; et al. Zero Thermal Expansion in Magnetic and Metallic Tb(Co,Fe)₂ Intermetallic Compounds. *J. Am. Chem. Soc.* **2018**, *140*, 602–605. [[CrossRef](#)]
13. Halder, M.; Yusuf, S.M.; Mukadam, M.D.; Shashikala, K. Magnetocaloric effect and critical behavior near the paramagnetic to ferrimagnetic phase transition temperature in TbCo_{2-x}Fe_x. *Phys. Rev. B* **2010**, *81*, 174402. [[CrossRef](#)]
14. Zhou, C.; Bao, H.; Matsushita, Y.; Chang, T.; Chen, K.; Zhang, Y.; Tian, F.; Zuo, W.; Song, X.; Yang, S.; et al. Thermal Expansion and Magnetostriction of Laves-Phase Alloys: Fingerprints of Ferrimagnetic Phase Transitions. *Materials* **2019**, *12*, 1755. [[CrossRef](#)] [[PubMed](#)]
15. Hirosawa, S.; Nakamura, Y. 59Co NMR Study of Spin Orientation in Pseudobinary Tb_{1-x}Dy_xCo₂. *J. Phys. Soc. Jpn.* **1982**, *51*, 1162–1165. [[CrossRef](#)]
16. Gu, K.; Li, J.; Ao, W.; Jian, Y.; Tang, J. The magnetocaloric effect in (Dy,Tb)Co₂ alloys. *J. Alloys Compd.* **2007**, *441*, 39–42. [[CrossRef](#)]
17. Zhuang, Y.; Xiang, C.H.; Kaiwen, Z.H.; Kefeng, L.I.; Chunhua, M.A. Phase structure and magnetocaloric effect of (Tb_{1-x}Dy_x)Co₂ alloys. *J. Rare Earths* **2008**, *26*, 749–752. [[CrossRef](#)]
18. Zhang, D.; Ma, X.; Yang, S.; Song, X. Role of the electronic structure in the morphotropic phase boundary of Tb_xDy_{1-x}Co₂ studied by first-principle calculation. *J. Alloys Compd.* **2016**, *689*, 1083–1087. [[CrossRef](#)]
19. Palit, M.; Pandian, S.; Chattopadhyay, K. Phase relationships and magnetic properties of Tb_xDy_{1-x}Fe_{1.95} alloys. *J. Alloys Compd.* **2012**, *541*, 297–304. [[CrossRef](#)]
20. Ma, T.; Zhang, C.; Zhang, P.; Yan, M. Effect of magnetic annealing on magnetostrictive performance of a <110> oriented crystal Tb_{0.3}Dy_{0.7}Fe_{1.95}. *J. Magn. Magn. Mater.* **2010**, *322*, 1889–1893. [[CrossRef](#)]

21. Arout Chelvane, J.; Palit, M.; Basumatary, H.; Pandian, S.; Chandrasekaran, V. Structural, magnetic and Mössbauer studies on magnetostrictive $\text{Ho}_{1-x}\text{Tb}_x\text{Fe}_{1.95}$ [$x = 0-1$]. *Phys. B Condens. Matter* **2009**, *404*, 1432–1436. [[CrossRef](#)]
22. Liu, X.; Lin, K.; Gao, Q.; Zhu, H.; Li, Q.; Cao, Y.; Liu, Z.; You, L.; Chen, J.; Ren, Y.; et al. Structure and Phase Transformation in the Giant Magnetostriction Laves-Phase SmFe_2 . *Inorg. Chem.* **2018**, *57*, 689–694. [[CrossRef](#)]
23. Murtaza, A.; Zuo, W.; Yaseen, M.; Ghani, A.; Saeed, A.; Hao, C.; Mi, J.; Li, Y.; Chang, T.; Wang, L.; et al. Magnetocaloric effect in the vicinity of the magnetic phase transition in $\text{NdCo}_{2-x}\text{Fe}_x$ compounds. *Phys. Rev. B* **2020**, *101*, 214427. [[CrossRef](#)]
24. Murtaza, A.; Li, Y.; Mi, J.; Zuo, W.; Ghani, A.; Dai, Z.; Yao, K.; Hao, C.; Yaseen, M.; Saeed, A.; et al. Spin configuration, magnetic and magnetostrictive properties of $\text{Tb}_{0.27}\text{Dy}_{0.73-x}\text{Nd}_x\text{Fe}_2$ compounds. *Mater. Chem. Phys.* **2020**, *249*, 122951. [[CrossRef](#)]
25. Murtaza, A.; Yang, S.; Khan, M.T.; Ghani, A.; Zhou, C.; Song, X. Temperature dependent magnetization and coercivity in morphotropic phase boundary involved ferromagnetic $\text{Tb}_{1-x}\text{Gd}_x\text{Fe}_2$ system. *Mater. Chem. Phys.* **2018**, *217*, 278–284. [[CrossRef](#)]
26. Chang, T.Y.; Zhou, C.; Mi, J.; Chen, K.; Tian, F.; Chen, Y.S.; Wang, S.G.; Ren, Y.; Brown, D.E.; Song, X.; et al. Crystal structures and phase relationships in magnetostrictive $\text{Tb}_{1-x}\text{Dy}_x\text{Co}_2$ system. *J. Phys.-Condens. Matter* **2020**, *32*, 135802. [[CrossRef](#)]
27. Yang, S.; Ren, X. Noncubic crystallographic symmetry of a cubic ferromagnet: Simultaneous structural change at the ferromagnetic transition. *Phys. Rev. B* **2008**, *77*, 014407. [[CrossRef](#)]
28. Ouyang, Z.W.; Wang, F.; Hang, Q.; Liu, W.; Liu, G.; Lynn, J.; Liang, J.; Rao, G. Temperature dependent neutron powder diffraction study of the Laves phase compound TbCo_2 . *J. Alloys Compd.* **2005**, *390*, 21–25. [[CrossRef](#)]
29. Stein, F.; Leineweber, A. Laves phases: A review of their functional and structural applications and an improved fundamental understanding of stability and properties. *J. Mater. Sci.* **2021**, *56*, 5321–5427.
30. Atzmony, U.; Dublon, G. Directions of easy magnetization in Laves RCO_2 compounds. *Phys. B+C* **1977**, *86–88*, 167–168. [[CrossRef](#)]
31. Horner, H.; Varma, C.M. Nature of Spin-Reorientation Transitions. *Phys. Rev. Lett.* **1968**, *20*, 845–846. [[CrossRef](#)]
32. Atzmony, U.; Dariel, M.P.; Bauminger, E.R.; Lebenbaum, D.; Nowik, I.; Ofer, S. Spin-Orientation Diagrams and Magnetic Anisotropy of Rare-Earth-Iron Ternary Cubic Laves Compounds. *Phys. Rev. B* **1973**, *7*, 4220–4232. [[CrossRef](#)]
33. Duc, N.H. Effects of the 3d–5d Hybridization on the 4f–3d Coupling in the Rare Earth–Transition Metal Compounds. *Phys. Status Solidi (B)* **1993**, *175*, K63–K66. [[CrossRef](#)]
34. Liu, J.-J.; Ren, W.J.; Li, D.; Sun, N.K.; Zhao, X.G.; Li, J.; Zhang, Z.D. Magnetic transitions and magnetostrictive properties of $\text{Tb}_x\text{Dy}_{1-x}(\text{Fe}_{0.8}\text{Co}_{0.2})_2$ ($0.20 < x < 0.40$). *Phys. Rev. B* **2007**, *75*, 064429.
35. Chikazumi, S.; Chikazumi, S.; Graham, C.D. *Physics of Ferromagnetism*, 2nd ed.; Oxford University Press: Oxford, UK, 1997; p. 503.
36. Atzmony, U.; Dariel, M.P.; Bauminger, E.R.; Lebenbaum, D.; Nowik, I.; Ofer, S. Magnetic anisotropy and spin rotations in cubic laves compounds, anisotropy and spin rotations in cubic laves compounds. *Phys. Rev. Lett.* **1972**, *28*, 244. [[CrossRef](#)]
37. Hu, C.-C.; Yang, T.N.; Huang, H.B.; Hu, J.M.; Wang, J.J.; Shi, Y.G.; Shi, D.N.; Chen, L.Q. Phase-field simulation of domain structures and magnetostrictive response in $\text{Tb}_{1-x}\text{Dy}_x\text{Fe}_2$ alloys near morphotropic phase boundary. *Appl. Phys. Lett.* **2016**, *108*, 141908. [[CrossRef](#)]
38. Ma, T.; Liu, X.; Pan, X.; Li, X.; Jiang, Y.; Yan, M.; Li, H.; Fang, M.; Ren, X. Local rhombohedral symmetry in $\text{Tb}_{0.3}\text{Dy}_{0.7}\text{Fe}_2$ near the morphotropic phase boundary. *Appl. Phys. Lett.* **2014**, *105*, 192407. [[CrossRef](#)]
39. Clark, A.; Crowder, D. High temperature magnetostriction of TbFe_2 and $\text{Tb}_{0.27}\text{Dy}_{0.73}\text{Fe}_2$. *IEEE Trans. Magn.* **1985**, *21*, 1945–1947. [[CrossRef](#)]
40. Deng, C.G.; Ye, L.; He, C.; Xu, G.; Zhai, Q.; Luo, H.; Liu, Y.; Bell, A.J. Reporting Excellent Transverse Piezoelectric and Electro-Optic Effects in Transparent Rhombohedral PMN-PT Single Crystal by Engineered Domains. *Adv. Mater.* **2021**, *33*, 2103013. [[CrossRef](#)] [[PubMed](#)]